DIGITAL IMAGING FOR PROCESS MONITORING AND CONTROL WITH INDUSTRIAL APPLICATIONS

Honglu Yu , John F. MacGregor

McMaster Advanced Control Consortium
Department of Chemical Engineering
McMaster University, Hamilton, On. Canada

Abstract: The development of on-line digital imaging systems for process monitoring and control is illustrated through two industrial applications: i) the control of coating concentration and distribution on snack food products, and ii) the monitoring of boiler systems through imaging of the combustion processes. Feature information extracted from images using Multivariate Image Analysis (MIA) based on Principal Component Analysis (PCA), is used to develop models to predict product quality and process property variables. The imaging systems are used to monitor these product quality and process property variables, to detect and diagnose operational problems in the plants, and to directly implement closed-loop feedback control.

Keywords: Multivariate Image Analysis, Principal Component Analysis, Partial Least Square, Snack Food, Flame, Combustion,

1. INTRODUCTION

The availability of informative, inexpensive, and robust on-line sensors is one of the most important factors for the successful monitoring and control of processes. The petrochemical industry made rapid advances in multivariable model predictive control largely because they had the availability and abundance of inexpensive and informative sensors such as thermocouples, pressure transducers, flow meters, pH and ion-specific meters and gas chromatographs. This is a direct result of the fact that the major streams in petrochemical processes consist of well mixed gases and liquids which made the use of such sensors very easy. On the other hand, the solids processing industry has had much less success at implementing advanced control precisely because of the lack of such sensors. In industries that produce solid products, generally product properties are measured periodically by manually collecting samples and then analyzing them in the laboratory. The analysis procedure often requires that the samples be destroyed and the procedures are time consuming and manpower intensive. However, with the advent of inexpensive digital cameras over the past decade, things are changing rapidly. Today an RGB color camera connected to a fairly powerful PC is on the order of only a few thousand dollars or so. In contrast, to insert a simple thermocouple well into a process line or a reactor is considerably more expensive. If affordable digital imaging systems can be used to effectively extract subtle information on the behavior of a process or on the quality of the product, then it could indeed lead to a more rapid application of advanced control in process industries manufacturing solid products such as pulp and paper, polymer sheet and films, and food products.

Much of the literature on digital image processing involves methods for altering the visual image in some way in order to make it more visually appealing, or to extract information on the shapes, boundaries or location of various observable features. In this sense traditional image processing techniques (Ross et. al., 2001; Stojanovic et. al., 2001; Katafuchi et. al., 2000) serve as automated vision systems performing operations faster and more precisely than human operators. These are indeed a very important class of problems. However, many quality monitoring and control problems are more similar to

those treated in this paper. They do not involve image enhancement issues, but rather the extraction of subtle information from the image (much of which is not readily visible to the human eye) that is related to product quality. Two examples are treated in this paper: prediction of the average coating concentrations and the distribution of the coating on snack food products passing on a moving belt under the imaging system, and the prediction of the heating content of the waste fuel stream and the NOx and SO_2 concentration in the off-gas generated in a boiler system. In these situations image processing is not concerned with image enhancement or even with the image space at all. Rather, the problem is one of information extraction from the image and the use of such information for prediction, monitoring and control. For this purpose a different set of techniques falling under the heading of multivariate image analysis (MIA) (Esbensen and Geladi, 1989; Geladi and Grahn, 1996) which employs multivariate statistical techniques such as Principal Component Analysis (PCA) and Partial Least Squares (PLS) have been developed. In this approach most of the analysis is done in the latent variable feature space rather than in the image space. Although most of the MIA methods have been applied to the analysis of single still images, an indication of their potential for monitoring time varying images was presented by Bharati and MacGregor (1998), and subsequently applied to the on-line monitoring of lumber defects (Bharati and MacGregor, 2003), and pulp and paper quality (Bharati and MacGregor, 2003). In this paper we report on the development of two industrial on-line imaging systems. The first is for the extraction of coating content and distribution from time varying images of snack food products, and for the on-line monitoring and control of the industrial snack food product lines. In the second, a feature extraction method is presented for monitoring the combustion process in a boiler system using color flame images. More detals can be found in Yu and MacGregor (2003a), Yu et. al. (2002) and Yu and MacGregor (2003b).

2. BASIC THEORY OF MIA

In the most commonly used electronic cameras, the color of each pixel is characterized by the numerical values (normally integers from 0 to 255) of its red, green and blue (RGB) channels. Therefore, a color image can be expressed as a 3-way matrix. Two ways are the spatial coordinates and the third way is the color channel. Without considering the spatial coordinates of the pixels, we can unfold the image matrix and express it as a 2-way matrix. In this paper, the feature variables extracted are computed in PCA score space obtained using Multivariate Image Analysis (MIA) techniques (Geladi and Grahn, 1996).

Without considering the spatial coordinates of pixels, we can unfold the image matrix and express it as a 2-way matrix. MPCA is equivalent to performing PCA on this unfolded image matrix **I**.

$$\mathbf{I} = \sum_{k=1}^{K} \mathbf{t}_k \mathbf{p}_k^{\,T} + \mathbf{E}$$

where K is the number of principal components, the $\mathbf{t}_k$'s are score vectors and the corresponding $\mathbf{p}_k$'s are loading vectors. For RGB color image, the maximum number of principal components is 3.

A kernel algorithm is used to compute the loading vectors. In this algorithm a kernel matrix ($\mathbf{I}^T\mathbf{I}$) is first formed (for a set of images, kernel matrix is calculated as the summation of individual kernel matrix for each image), and then singular value decomposition (SVD) is performed on this very low dimension matrix (3×3 for an RGB color image) to obtain loading vectors $\mathbf{p}_a$ (a=1,…K).

After obtaining loading vectors, the corresponding score vectors $\mathbf{t}_k$ are then computed via $\mathbf{t}_k=\mathbf{I}\mathbf{p}_k$. $\mathbf{t}_k$ is a long vector with length N (N is the number of total pixels in the image). After proper scaling and round off, it can be refolded into the original image size and displayed as an image.

$$s_{k,i} = \mathrm{Round}\left(\frac{t_{k,i} - t_{k,\min}}{t_{k,\max} - t_{k,\min}} \times 255 \right),\ i=1,\ldots,N$$

$$(\mathbf{s}_k)_{N\times 1} \xrightarrow{refold} (\mathbf{T}_k)_{Nrow\times Ncol}$$

$\mathbf{T}_k$ is the score image of component k. The values of $\mathbf{T}_k$ are integers from 0 to 255. It should be pointed out that when many images are studied, a common scaling range ($t_{k,\min}$ and $t_{k,\max}$) should be used for all the images.

Since the first two components explain most of the variance, instead of working in original 3-dimensional RGB space, working in the t_1-t_2 score space allows us interpret the images much easier.

Inspection on t_1-t_2 score plot is a common tool in general PCA analysis to give an overview of the whole system. However, when the studied objects are images, because of large number of pixels many pixels would fall overlap each other in t_1-t_2 score plot. Therefore a 256×256 histogram, is used to describe t_1-t_2 score plot space in this situation (Geladi and Grahn, 1996) and a color coding scheme, in which a darker color indicates a lower intensity (black indicates no pixel falling) and a brighter color indicates a higher intensity, is used to indicate the intensity of the pixel locations in the score plot.

3. SNACK FOOD APPLICATION

3.1 Problem description

In this application the objective is to develop a model to prediction coating concentration and the distribution of the coating coverage on the snack food products.

The first step is to collect an adequate dataset. A successful model requires a set of sample images

including both uncoated and coated product samples with varied coating levels. For each coated product image, the corresponding average coating is obtained by lab analysis of the product. 110 images are collected from the on-line camera system and grab samples corresponding to those images are taken to the lab for analysis. Half of them are used as a training dataset and another half are used as a test set The images are all 480×640 RGB color images, with 256 intensity levels in each channel. Some sample images are shown in Figure 1.

Uncoated Low-coated High-coated

Figure 1 Sample snack food images

3.2 Methodology

Let us consider a data set of color images and the corresponding lab analyzed average coating concentrations. A model to predict coating concentration can be obtained by regressing features extracted from the images against the corresponding average coating concentrations. In this research, Partial Least Squares regression (PLS) is employed because of the high correlation among the feature variables.

Feature extraction is a critical step to achieve good prediction results. In Yu and MacGregor (2003a), six feature extraction methods (including 2 overall feature methods and 4 distribution feature methods) are compared and discussed. Examples show that for predicting the average coating level of the whole image, all six methods can achieve good results. However, when predicting the coating level from small sub-images, only one method (method 6) exhibits sufficient robustness in prediction (Yu and MacGregor, 2003a). This method will be briefly introduced in the following.

The method first starts with a fine (256×256) histogram in the t_1-t_2 color space, and then lumps the elements in that space into histogram bins that are expected to contain similar values of coating concentration. In order to define histogram bin classes in the score space that contain pixels having similar coating content, two covariance plots are computed between the counts in the histogram bins and two variables, z_1 and z_2, related to the average coating concentrations in the images.

$$\mathbf{z}_1 = \begin{bmatrix} \bar{y}_{I_1} \\ \bar{y}_{I_2} \\ \mathbf{M} \\ \bar{y}_{I_K} \end{bmatrix}, \quad \mathbf{z}_2 = \left|\mathbf{z}_1 - y^*\right| = \begin{bmatrix} \left|\bar{y}_{I_1} - y^*\right| \\ \left|\bar{y}_{I_2} - y^*\right| \\ \mathbf{M} \\ \left|\bar{y}_{I_K} - y^*\right| \end{bmatrix}$$

$$y^* = \frac{\max(\bar{y}) + \min(\bar{y})}{2}$$

Two covariance plots were necessary in order to obtain a unique or one-to-one correspondence between the bin classes and coating content (Yu and MacGregor, 2003a). For each (t_1, t_2) location, a phase angle can be computed for the observed point in the space of the two covariance values. Therefore an angle plot can be obtained in which similar angle values indicate similar coating content. Figure 2 is the color-coded angle plot in the t_1-t_2 space. 32 bins are selected based on angle values. Image pixels having (t_1,t_2) values falling within the same bin should have similar coating levels. Then, a one-dimensional histogram can be formed for each image by counting the number of pixels falling in each bin. The final feature variables are chosen as the 32 values of the cumulative histogram (Yu and MacGregor, 2003a).

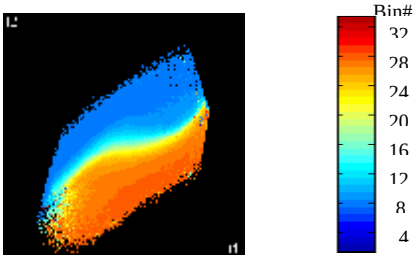

Figure 2 Color coded angle plot in t_1-t_2 space, with 32 bins based on angle values

Once the feature variables have been obtained we can build inferential models by regressing these feature variables against the laboratory coating concentration for the training set. PLS regression is used because the feature data is highly correlated, and because it permits for validation of data from new images.

After obtaining the PLS model using the training data set, the prediction performance of the model was evaluated against the test data sets. Figure 3 plots the predicted average coating level vs. the lab analysis data. The fit of the training data is very good, and the prediction of the new test data is almost equally good.

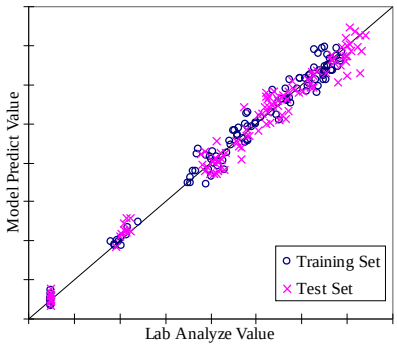

Figure 3 Predicted vs. observed coating content

To obtain a prediction for each new image the product pixels are projected onto the t_1-t_2 plane obtained by the PCA model. By counting the number of pixels falling into each of the bins (Figure 3), we obtain the 32 bin cumulative one-dimensional histogram to be used as regressor variables in the

PLS model. Average coating level is then predicted by the PLS model.

The method developed above is almost independent of the image size (Yu and MacGregor, 2003a). Therefore, the coating distribution can be estimated by a small window strategy (Yu and MacGregor, 2003a). In this small window strategy, the image is divided into many small pieces (see Figure 4), and the coating distribution is obtained by calculating the average coating concentration for each sub-image. Variance of the coating distribution can be estimated from this distribution and used for on-line monitoring. See Yu and MacGregor (2003a) for further details on this and other approaches for estimating the coating distribution.

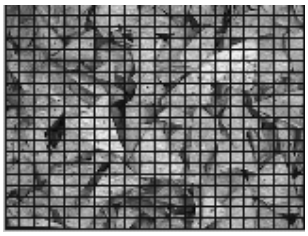

Figure 4 An image divided into 20×20 windows

3.3 On-line results

The model developed has been successfully implemented on the industrial production lines. Some on-line results are presented in this section. More results can be found in Yu et. al. (2003).

Some of the first data collected from the imaging system are shown in the upper plot in Figure 5. The raw coating predictions are shown by the light gray line. For this evaluation study frequent grab samples were taken every 5 minutes and analyzed later in the lab. These are shown as circles in the Figure 5. One can see that the predicted coating concentrations from the images are in good agreement with the lab analysis. However, the image predictions reveal a clear saw-tooth behavior in the concentration that is not evident only from the lab data, even during this fast sampling program. This unexpected result was explained by the coating hopper refilling operations in the process. The lower plot in Figure 5 shows the signal of the motor of the hopper refilling system. As the level of the coating powder in the feed hopper falls to a certain level, the motor is activated to refill the hopper. The level of coating inside hopper then increases rapidly. Clearly Figure 5 shows that the discharge of rate of coating from the hopper to the coating operation (tumbler) is a strong function of the coating level in the hopper.

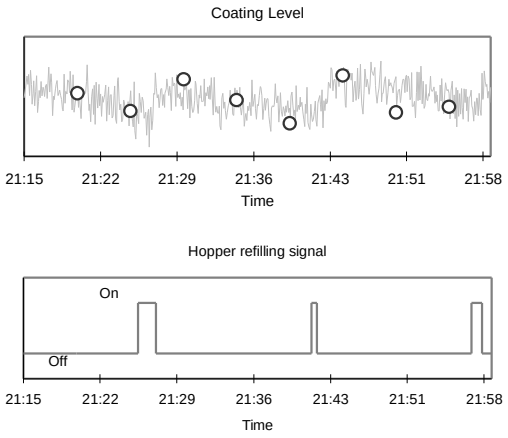

Figure 5 Detection of hopper effect

Figure 6 shows a 4 hour on-line monitoring period for the product. Shown are the predicted coating level (1), the uncoated product weight (2), the coating feeder speed (3) and the signal of the dump gate (4). During this period, at about time 19:35, the feed rate of the non-coated product to the tumbler suddenly increased and, as the result of ratio control, the coating feeder speed also increased. However, the coating feeder speed was limited by its maximum capacity and could not feed coating fast enough to keep the desired ratio to the uncoated product. Therefore, the coating level on product decreased from the desired value. A second problem also occurred starting at about time 20:40 where the coating level suddenly started to continuously decrease. This occurred because the coating hopper was not set to automatic refilling mode and was therefore being depleted of coating. The result was that eventually no coating was being fed to the tumbler the dump gate had to open to remove the uncoated products from the belt. It should be pointed out that by looking only at process data (uncoated product weight and coating feeder speed) this fault was not detectable.

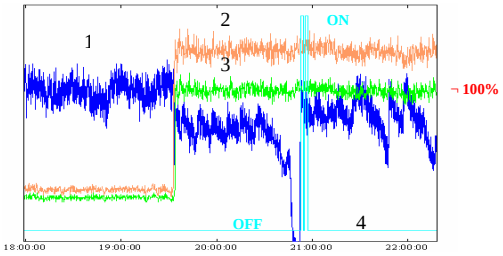

1 — Predicted coating level
2 — Uncoated product weight
3 — Coating feeder speed
4 — Dump gate open signal

Figure 6 On-line monitoring example

In Figure 7, operating data under closed-loop control covering a period of 24 hours is shown. Shown are the coating level set point and the predicted coating level (1), the uncoated product weight (2), the

coating feeder speed and the coating level bias change (4). In the employed control scheme, coating feeder speed is the manipulated variable and computed as the summation of the outputs of two controllers: a ratio controller for compensating variation of the uncoated product weight, and a feedback controller. The coating level bias is the output of the feedback controller. From Figure 7, we can see that the coating level successfully tracked the set point. Another point to note from this figure is that we can no longer see the saw-tooth effect of the coating feeder system that was apparent in Figures 5 and 6. This is because an operational change was introduced to eliminate this effect.

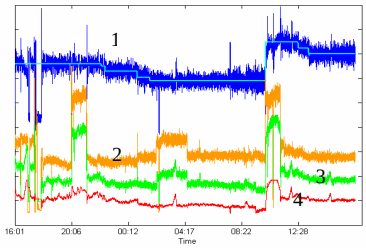

1 —— Predicted coating level (the lighter grey line shown in the middle is the coating level set point
2 —— Uncoated product weight
3 —— Coating feeder speed
4 —— Coating level bias

Figure 7 Closed-loop control

4. MONTITORING THE COMBUSTION PROCESS IN A BOILER SYSTEM

4.1 Process description

The steam boiler studied in this research uses both the waste liquid streams from other processes and natural gas as fuels. Therefore the overall composition of the fuel then often changes dramatically. One of the problems we studied in this application is then to predict the heat of combustion of the liquid waste fuel. An analog color camera has been installed in the boiler and is connected with a monitor for displaying the live images. In this research, the analog signals were recorded by a normal VCR and then a video card converted the signals on the video tapes into the digital images. The resulting images are RGB color images, with the size of 120×160 pixels. Considering the processing time, the imaging sample time is set as 1 frame per second.

Two case studies are presented in this paper. Case I covers a 114 minute period (see Figure 8). In this period of time, only liquid fuel is used. In the first half of this period of time, the liquid fuel flow rate decreases from 1.5 to 0.75 kg/s; then in the second half of the period, it increases back to 1.5 kg/s. The steam generated followed the same trend as the fuel flow. Case study I mainly used to illustrate that stable information can be obtained in the PCA t1-t2 score space even in image space the flame images are always bouncing around.

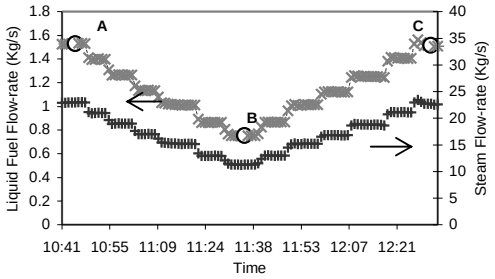

Figure 8 Flow rates of liquid fuel and steam for Case study I

Case II consists 12 video tapes collected during 2 month period of time. On each video tape a half an hour of flame images were recorded. The average process variables during the time when the video tapes were recorded were also collected. Both liquid fuel and natural gas flow rates, as well as the composition of liquid fuel were changing dramatically during that period of time. The objective is to predict the heat of combustion of liquid fuel and the NO_x and SO_2 concentration in the off-gas generated from the boiler system.

4.2 Case study I

A total of 6840 frame images are obtained for Case study I. In Figure 9, some sample images are shown corresponding to the points (A, B and C) marked in Figure 8. For each point, two consecutive images with 1 second time difference are shown. It is reasonable to assume that during this one second, the feed and composition conditions in the combustion process did not change. It can be observed that the flames in the boiler appeared highly turbulent, with the images changing significantly over every 1 second interval. This poses considerable difficulty in trying to extract stable information about the combustion process.

Table 1 Sample flame images taken one second apart at different conditions

A	B	C
		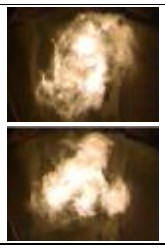

100 images are used in this study to compute the loading matrix and score scaling range. The first two components explained 99% of the total variance.

Table 2 shows the corresponding t1-t2 score plots for the sample images shown in Table 1. We can see

from Table 2 that for images captured at the same combustion condition (i.e. in the same columns in Table 1), the score plot histograms of pixel intensities are very similar. However, as the combustion conditions change (i.e. along rows), the locations of pixels in the score plots change noticeably. This is the key result that enables one to use flame images to analyze and monitor the process for changing conditions. For any given process condition, even though the flame images are bouncing around, the PCA score space of that image is very stable, and it only changes shape and location with changing process conditions.

Table 2 Score plots for the sample images shown in Table 1 (order is the same)

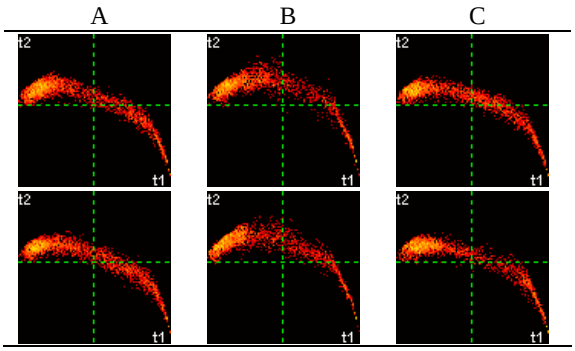

However, directly monitoring the process based on the appearance of the score plot is not practical. This is because it is hard for people to monitor a time series process by watching changes in a two dimensional matrix, and even if people were able to detect some changes happening in the score plot, it is hard to interpret such changes. Therefore, we need to extract features from the score plot that have more physical meaning and to further relate those features with the process variables to help us understand more about the combustion process and use these information to monitor the operating performance and emissions from these combustion processes.

4.3 Case study II

In Case study II, nine feature variables are extracted from the t1-t2 score plots of the flame images. These feature variables include four luminous features: flame luminous region area, flame brightness, uniformity of flame brightness and the average brightness of non-luminous area; and five color features: average t1 and t2 values of the whole image, average t1 and t2 values of the flame luminous region and the number of colors appearing in the flame region.

The flame luminous region is extracted from the image by choosing a mask in the score plot. The boundary of the mask is easily obtained by a trial and error process, whereby one selects a mask area in the score plot, selects the pixels lying under it and highlights them in the image space, and iterates until one obtains a mask that segments the feature of interest. The final mask selected for extracting the flame luminous region is shown as the green area in Figure 9a. To illustrate the segmentation ability of the mask a sample flame image is shown in Figure 9b. If we set all pixels falling outside this mask to have a gray color, the image shown in Figure 9c is obtained. We can see that the luminous flame region is separated from the other part of the image.

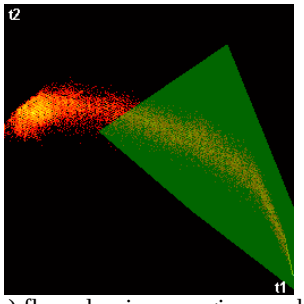

(a) flame luminous region mask

(b) one frame image

(c) separated flame

Figure 9 An illustration of flame luminous region mask

The detailed computation of the feature variables can be found in Yu and MacGregor (2003b). An average feature vector is used to represent the image data of each tape. PLS is used for regressing image feature variables against the property variables.

A PLS model is built to predict the product of heat of combustion and the liquid fuel flow rate. The heat of combustion can then be obtained by dividing the PLS model prediction by the liquid fuel flow rate. Other than the feature variables, the flow rates of liquid fuel and natural gas are used as the predictors This is shown in equation:

$$\hat{Q} = [F_{lf} \;\; F_{ng} \;\; \mathbf{v}] \cdot \hat{\boldsymbol{\gamma}}, \text{ where } Q = H_{Lf} \cdot F_{Lf}$$
$$\hat{H}_{lf} = \hat{Q} / F_{lf}$$

where $\mathbf{v}$ is the feature vector extracted from the image data, F_{ng} is the natural gas flow rate, F_{lf} is the flow rate of liquid fuel, $\hat{\boldsymbol{\gamma}}$ is the model regression coefficient vector and H_{Lf} is the heat of combustion.

10 samples are used as a training set and 2 samples are used as a test set. 6 latent variables and 8 latent variables are selected by cross validation. Figure 10 shows the prediction vs. observation plots for both models. We can see that the model has good prediction performance.

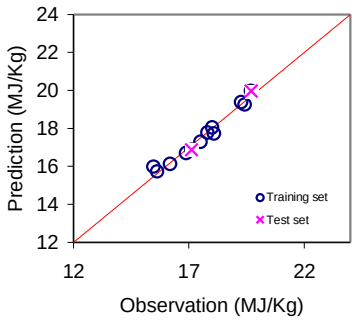

Figure 10 Prediction vs. observation plot for prediction of the heat of combustion of the liquid fuel

Two PLS models are developed to predict the emissive concentrations of NO_x and SO_2 respectively. For predicting each of the concentrations, three types of predictors are considered: i) using only process variables; ii) using only feature variables extracted from image data; and iii) using both types of variables. The process variables used here include temperature of the feed oxygen, and the flow rates of liquid fuel, natural gas, oxygen and steam. These models (6 in total) are listed in Table 3. For each model, 10 samples are used as a training set while 2 samples are used for evaluation (test set).

Table 3 Six models for predictions of NO_x and SO_2 concentration in off-gas generated

Predictors	Responses	
	NO_x	SO_2
Process variables	M_NO_x_1	M_SO_2_1
Feature variables from image data	M_NO_x_2	M_SO_2_2
Both process variables and feature variables from image data	M_NO_x_3	M_SO_2_3

Table 4 Summary for the six models for prediction of emission NO_x and SO_2 concentration

	Number of LV's	RMSEP for training set	RMSEP for test set
M_NO_x_1	5	18.97	19.96
M_NO_x_2	6	9.10	15.47
M_NO_x_3	7	13.12	25.83
M_SO_2_1	1	3.94	3.11
M_SO_2_2	7	0.41	0.27
M_SO_2_3	8	0.29	2.72

The number of latent variables (determined by cross validation) and RMSEP for both training set and test set of each of the six models are listed in Table 4. We can see that the best models are obtained by using only the feature variables extracted from the image data as predictors. By using process data, it seems that model predictions are not improved.

The prediction vs. observation plot for M_NOx_2 and M_SO2_2 (using only the feature variables extracted from the image data) are shown in Figure 11. The results show good agreement between the predicted and the measured data.

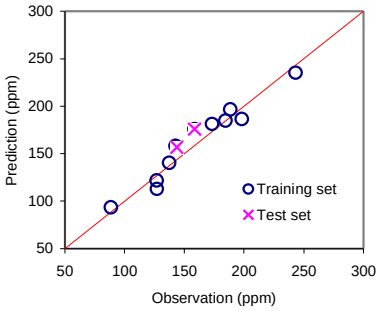

(a) NO_x concentration

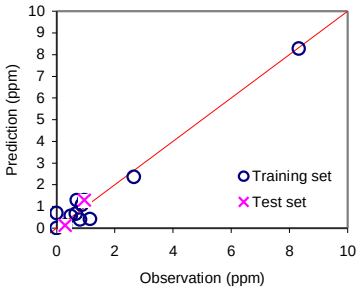

(b) SO_2 concentration

Figure 11 Prediction vs. Observation for NO_x and SO_2 concentrations

5. SUMMARY AND CONCLUSIONS

Development of on-line digital imaging systems for process monitoring and control are illustrated using two industrial applications.

The first application is to an industrial snack food production process. In this application, an inferential sensor based on RGB color images for measuring the coating content and distribution of the coating coverage of snack foods is developed and is implemented for on-line control of the industrial production line. Several plant tests show clearly that the coating concentration variations can be tracked by the image-based sensor, that process problems can be detected and that good results of closed-loop feed back control can be achieved.

The second industrial application involves monitoring turbulent flames in an industrial boiler. It has been shown that in t_1-t_2 score plot space computed from PCA; fairly stable information can be obtained even though in the image space, the flame is always bouncing around. A mask is selected in t_1-t_2

score plot to indicate the location of flame luminous area. Nine feature variables, including four luminous features and five color features, are extracted from each flame image. PLS models are built using these image feature variables to successfully predict the heat of combustion of the liquid waste fuel stream and the NO_x and SO_2 concentrations in the off-gas generated from the boiler system. This reveals the great potential for utilizing the flame images in combustion processes.

REFERENCES

Bharati, M. (2002) Multivariate Image Analysis for Process Monitoring and Control. Ph. D. thesis

Bharati, M.; J. F. MacGregor (1998) Multivariate Image Analysis for Real-Time Process Monitoring and Control. *Ind. Eng. Chem. Res.*, **37**, 4715

Esbensen, K.; P. Geladi (1989) Strategy of Multivariate Image Analysis (MIA). *Chemometrics and Intelligent Laboratory Systems*, **7**, 67

Geladi, P. and H. Grahn (1996). Multivariate Image Analysis. John Wiley & Sons, Chichester, England

Katafuchi, N.; M. Sano.; S. Ohara; M. Okudaira (2000) A Method for Inspecting Industrial Parts Surfaces Based on an Optics Model. *Machine Vision and Applications*, **12**, 170

Ross, B. J.; Fueten, F.; Yashkir, D. Y. (2001) Automatic Mineral Identification Using Genetic Programming. *Machine Vision and Applications* **13**, 61

Stojanovic, R.; Mitropulos, P.; Koulamas, C.; Karayiannis, Y.; Koubias, S. Real-Time Vision-Based System for Textile Fabric Inspection. Real-time Imaging 2001, **7**, 507

Yu, H. and J. F. MacGregor (2003a). Multivariate Image Analysis and Regression for Prediction of Coating Content and Distribution in the Production of Snack Foods. *Chemometrics and Intelligent Laboratory Systems*. Accepted

Yu, H., J. F. MacGregor, G. Haarsma and W. Bourg (2003). Digital Imaging for On-line Monitoring and Control of Industrial Snack Food Processes. Ind. Eng. Chem. Res. Accepted

Yu, H. and J. F. MacGregor (2003b). Monitoring Turbulent Nonpremixed Flames in an Industrial Boiler Using Multivariate Image Analysis (MIA). Submitted to *AIChE J.*